

ARTICLE OPEN



GENOMICS AND GENE THERAPY

Unraveling the molecular landscape of Erdheim–Chester disease: new insights from methylome and transcriptome integration

Miriam Cerván-Martín ¹✉, Francesco Pegoraro ^{2,3}, Javier Martínez-López ^{1,4}, Inmaculada Rodríguez-Martin ¹, Ana Márquez¹, Lourdes Ortiz-Fernández¹, Marialbert Acosta-Herrera ¹, Martin Kerick ¹, Eduardo Andrés-León ¹, Francesco Catamerò ⁵, Matthias Papo^{6,7}, Fleur Cohen-Aubart^{6,7}, Zahir Amoura^{6,7}, Julien Haroche ^{6,7}, Augusto Vaglio ^{8,9,10} and Javier Martín^{1,10}

© The Author(s) 2025

Erdheim–Chester Disease (ECD) is a rare histiocytosis characterized by a wide spectrum of clinical manifestations. Although somatic mutations have been involved in ECD, its etiology remains poorly understood. This study aimed to identify novel molecular mechanisms involved in ECD through the first integrated methylome and transcriptome analysis. Peripheral blood samples were collected from 137 ECD patients and 410 controls. Genome-wide DNA methylation and transcriptome analyses were performed, followed by functional in silico studies using different online bioinformatics tools. Subsequently, methylome and transcriptome data were integrated, and a drug repurposing approach was undertaken. Our results revealed 2511 differentially methylated positions and 1484 differentially expressed genes associated with ECD. The integrative analysis identified 46 alterations in DNA methylation patterns that regulate the expression levels of 29 altered genes in ECD patients, highlighting key genes involved in immune response and tumorigenesis. Remarkably, our results identified B cells and NF-κB signaling pathway as novel contributors of ECD pathogenesis. Finally, the drug repurposing analysis identified potential therapeutic options for ECD patients. In conclusion, this study represents an important advance in understanding the molecular basis of ECD, proposing novel cell types and pathways involved in ECD pathogenesis and suggesting new avenues for clinical management.

Leukemia; <https://doi.org/10.1038/s41375-025-02742-z>

INTRODUCTION

Erdheim–Chester disease (ECD) is a rare histiocytosis, with ~2000 cases recorded globally. It is characterized by foamy CD68⁺ and CD11a⁺ histiocyte tissue infiltration and manifests with a wide spectrum of clinical features, spanning from organ-limited to aggressive systemic forms [1]. ECD predominantly affects individuals aged 50 to 70 years, with a higher prevalence among males [2], but pediatric-onset ECD is also reported [3].

ECD is considered a myeloid neoplasm in which inflammation plays a pivotal role in the disease progression and the tissue damage [4, 5]. The identification of activating somatic mutations in several proto-oncogenes or genes regulating cell growth and proliferation has highlighted the crucial role of genetics in the development of the disease [1, 2, 4, 5]. Furthermore, the genetic predisposition to ECD has recently been investigated through a

genome-wide association study (GWAS), which led to the identification of the first germline variant associated with ECD risk [6]. This study reinforced the significant role of genetic factors in this condition and opened new perspectives on disease development. Nevertheless, the pathogenesis of ECD remains poorly understood, highlighting the need for different approaches to uncover the mechanisms driving this condition.

In recent years, there have been numerous efforts to examine the contribution of epigenetic mechanisms to complex diseases pathology, including neoplastic and immune-mediated inflammatory diseases (IMIDs) [7, 8]. Among epigenetic modifications, DNA methylation is the most extensively studied and has significantly advanced our understanding of how environmental factors can regulate gene expression [9]. Moreover, alterations in DNA methylation are associated with disease activity, clinical subtypes

¹Institute of Parasitology and Biomedicine López-Neyra, Spanish National Research Council, Granada, Spain. ²Department of Hematology and Oncology, Meyer Children's Hospital IRCCS, Florence, Italy. ³Department of Experimental and Clinical Medicine, University of Florence, Florence, Italy. ⁴Systemic Autoimmune Disease Unit, Hospital Clínico San Cecilio, Instituto de Investigación Biosanitaria Ibs. GRANADA, Granada, Spain. ⁵Department of Health Sciences, University of Florence, Florence, Italy. ⁶Sorbonne Université, Assistance Publique-Hôpitaux de Paris, Service de Médecine Interne, Paris, France. ⁷Centre National de Référence Maladies Systémiques Rares et Histiocytoses, Hôpital Pitié-Salpêtrière, Centre d'immunologie et des maladies infectieuses INSERM UMR51135, Paris, France. ⁸Nephrology and Dialysis Unit, Meyer Children's Hospital IRCCS, Florence, Italy. ⁹Department of Biomedical, Experimental and Clinical Sciences, University of Florence, Florence, Italy. ¹⁰These authors contributed equally: Augusto Vaglio, Javier Martín.

✉email: miriam.cervan@ipb.csic.es

Received: 7 May 2025 Revised: 2 July 2025 Accepted: 11 August 2025

Published online: 21 August 2025

and responses to drugs, making them amenable for use in clinical practice [10, 11]. In addition, the use of novel approaches integrating methylome and transcriptome data has provided insights into the pathogenesis of both hematological malignancies and IMiDs [12–14].

Considering all the above, we conducted the first analysis of the methylome and transcriptome in ECD, including the integration of these omics data, in a large ECD cohort, detecting a significant dysregulation in the epigenome and transcriptome of ECD patients. Our findings allowed the identification of new molecules and altered pathways that could help in the identification of novel biomarkers and therapeutic targets.

MATERIAL AND METHODS

Study population

A case-control cohort of European descent comprising a total of 137 individuals diagnosed with ECD and 410 unaffected controls was analyzed in this study. Informed written consent was signed by all participants in accordance with the tenets of the Declaration of Helsinki and all DNA samples were irreversibly anonymized. This study was approved by the CSIC Ethic Committee.

Blood samples from ECD patients were collected at two referral centers for ECD, namely the Pitié Salpêtrière Hospital (Paris, France) and the Meyer Children's Hospital IRCCS (Florence, Italy). Patients enrolled were diagnosed over the age of 55 and included 94 males and 42 females. All patients were diagnosed in accordance with the latest consensus guidelines for the diagnosis and management of ECD [15]. Data collected included demographics, diagnostic biopsy, mutational status, cardiovascular risk factors, organ involvement at any time, therapy and prognosis. The main clinical features of the analyzed ECD patients are included in Supplementary Table 1. Unaffected controls samples were obtained from the multi-center, cross-sectional, clinical study PRECISEADS [16]. Due to the relevance of BRAF^{V600E} mutation in ECD pathology, subgroups of patients were defined for the statistical analysis based on the mutational status (i.e., BRAF^{V600E}-positive and BRAF^{V600E}-negative patients) and the use of MAPK inhibitors as treatment at the time of sampling or in the previous 6 months (i.e., untreated BRAF^{V600E}-positive and treated BRAF^{V600E}-positive patients). The comparisons performed in the present study included: ECD patients vs. controls, BRAF^{V600E}-positive vs. BRAF^{V600E}-negative, BRAF^{V600E}-positive vs. controls, BRAF^{V600E}-negative vs. controls and untreated BRAF^{V600E}-positive vs. treated BRAF^{V600E}-positive patients. The specific sample sizes for each group are provided in Supplementary Table 2.

Genome-wide methylation assay and data processing

Whole peripheral blood samples were obtained from ECD patients and unaffected controls. After DNA extraction, bisulfite conversion was performed following the manufacturer's protocols. Subsequently, the genomes were amplified, fragmented and hybridized to the Infinium Methylation EPIC BeadChip (Illumina, San Diego, CA, USA), which has a coverage for more than 850,000 CpG sites at single-nucleotide resolution, including 99% of reference sequence (RefSeq) genes and 95% of CpG islands. A detailed explanation of the data processing is included in the Supplementary Material.

Differential DNA methylation analysis for all comparisons was performed using eBayes moderate t-test from the limma package [17]. The comparisons were carried out including demographic location, sex, age and cell composition as covariates. To correct for multiple testing, we used a false discovery rate (FDR). An additional filter based on beta value differences ($\Delta\beta$) between the compared groups was applied. Those probes with a $p\text{-value}_{\text{FDR}} < 0.01$ and $|\Delta\beta| > 0.15$ were considered as differentially methylated positions (DMPs).

RNA-seq and gene expression analysis

RNA sequencing data from all individuals were obtained from high quality whole blood RNA samples and 1 μg of each RNA sample was used for library synthesis according to the manufacturer's protocol. RNA sequencing data acquisition and processing are detailed in the Supplementary Material.

To identify differentially expressed genes (DEGs) in each comparison, we used DEcomposing heterogeneous Cohorts using Omic data profiling (DECO) [18]. This bioinformatic tool is specifically designed for analyzing heterogeneous cohorts. A more detailed explanation of DECO is included in the Supplementary Material.

Enrichment analysis of the associated signals

Several online enrichment tools were employed to prioritize the most relevant molecular processes involved in ECD pathogenesis. A detailed description of these tools can be found in the Supplementary Material.

Integrative analysis of DNA methylation and transcriptome data

To identify modifications on DNA methylation patterns that impact on gene expression regulation, a linear model was calculated using the MatrixEQTL R package [19]. A maximum distance of 1 Mb between CpG sites and genes was defined. To consider the influence of DNA methylation on gene expression as significant in ECD patients, we established the following criteria: (i) the CpG was differentially methylated in the DNA methylation analysis; (ii) the gene was differentially expressed in the transcriptomic analysis; and (iii) the CpG–gene interaction showed a significant association ($p\text{-value}_{\text{FDR}} < 0.05$) in the integrative analysis.

Drug repurposing of the integration results

Finally, we conducted a drug repurposing analysis to identify potential candidate drugs for ECD treatment using the DrugBank V.5.0 database [20]. We explored the proteins encoded by the genes identified in the integrative analysis as well as the proteins that interact with those proteins (interaction score > 0.7) according to STRING [21]. Approved drugs for IMiDs and/or neoplastic diseases were prioritized to identify the most promising options.

RESULTS

DNA methylation profiles differ between Erdheim–Chester disease patients and controls

After quality control (QC), a total of 784,676 CpG sites from a final cohort of 81 individuals with ECD and 176 unaffected controls were included in the methylation analysis (Supplementary Table 2). The results revealed 2512 DMPs, annotated to 1563 unique genes, across the whole genome (Fig. 1A, Supplementary Table 4). Among the DMPs, ~60% were hypermethylated, while the remaining 40% were hypomethylated in ECD cases compared to controls. Regarding their genomic location, most DMPs were found in OpenSea regions (54.30%) and CpG Islands (27.67%). Furthermore, we observed that DMPs located in or near promoter regions were more frequently hypomethylated (63.30%) than hypermethylated (19.20%) (Fig. 1B).

We identified DMPs mapped to novel candidate genes potentially involved in ECD pathogenesis, including genes associated with the RAS-RAF-MEK-ERK and PI3K-AKT-mTOR signaling pathways (Supplementary Table 5), which are known to play key roles in ECD development [4]. Moreover, we discovered altered methylation patterns associated with genes from the tumor necrosis factor (TNF) superfamily pathway, a key player in the pro-inflammatory cascade that characterizes ECD [2] (Supplementary Table 5). Changes on the methylation patterns of the *SETBP1* gene also showed a significant association in the case-control analysis (Supplementary Table 4). Notably, genetic variation at the *SETBP1* loci are related to ECD risk in the first and recent GWAS on ECD [6].

The gene ontology (GO) enrichment analysis revealed immune system-related pathways, including IgA binding, positive regulation of interleukin (IL)-5 production, and negative regulation of Fc-gamma receptor involved in phagocytosis. Additionally, we observed significant enrichment in pathways related to cell proliferation and growth, such as replication fork processing, DNA-dependent DNA replication fidelity maintenance, microtubule organizing center localization, and centrosome localization (Fig. 2, Supplementary Table 6). Furthermore, transcription factor (TF) analysis indicated that the DMPs were significantly enriched with TF binding sites that played significant roles in tumorigenic processes and had previously been associated with various cancers (Fig. 2, Supplementary Table 7). Interestingly, one of those enriched TFs was OCT2, which is primarily expressed in blood and immune cells, particularly in monocytes [22].

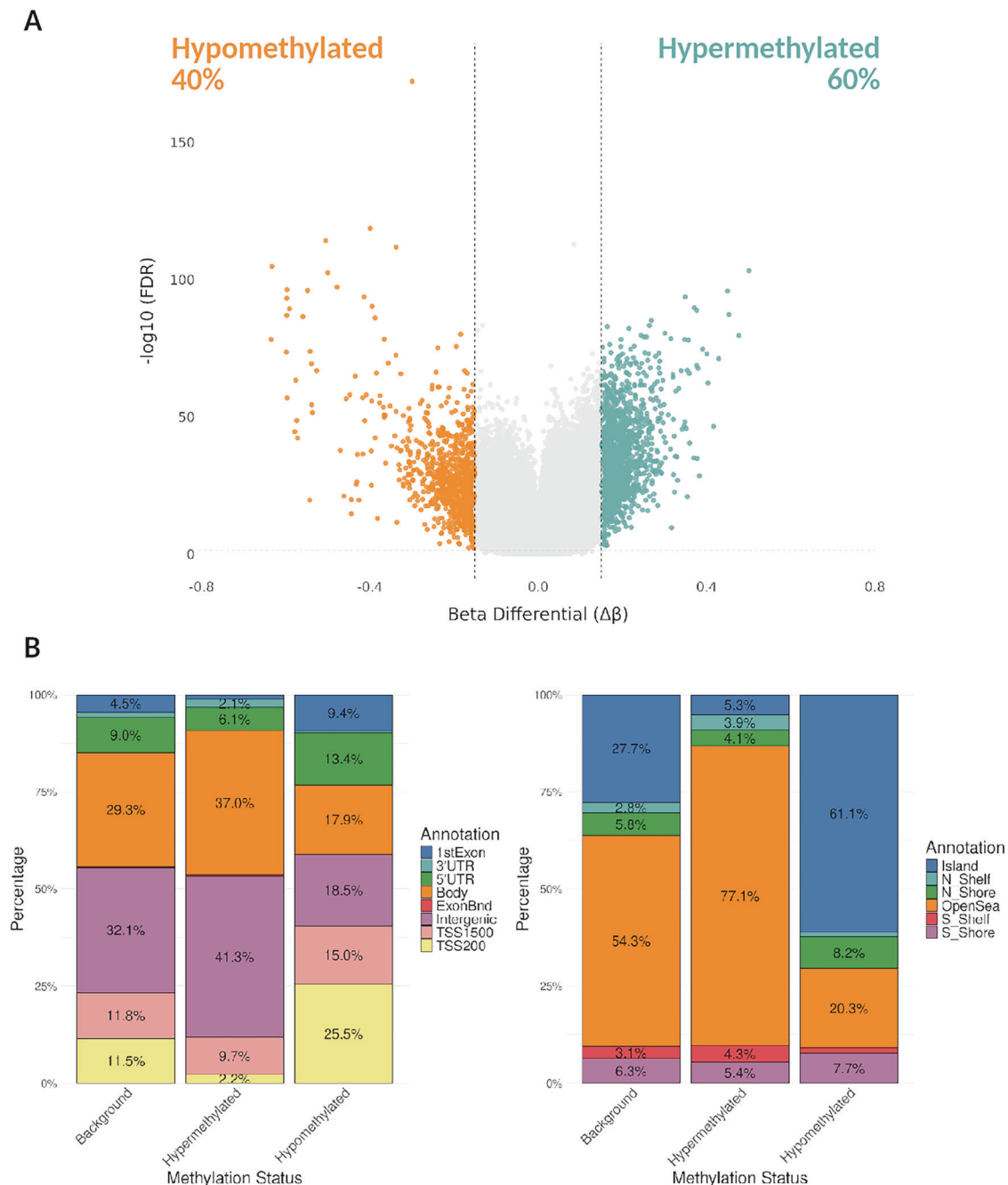


Fig. 1 Results from the comparison of DNA methylation patterns between patients with Erdheim-Chester disease and controls. **A** Volcano plot of the epigenome-wide association study results. False discovery rate (FDR) values are represented on the $-\log_{10}$ scale in the y-axis. The effect size and direction obtained for each CpG site is depicted in the x-axis through the beta differential ($\Delta\beta$) value. Significant threshold ($FDR < 0.05$ and $\Delta\beta > |0.15|$) is marked by the dashed lines. Orange and blue dots represent hypomethylated and hypermethylated differentially methylated positions (DMPs), respectively. **B** Bar plots representing the annotation of the significant hypomethylated and hypermethylated DMPs in relation to CpG island (right panel) and gene location (left panel). Promoter regions included TSS1500, TSS200, 1stExon and 5'UTR.

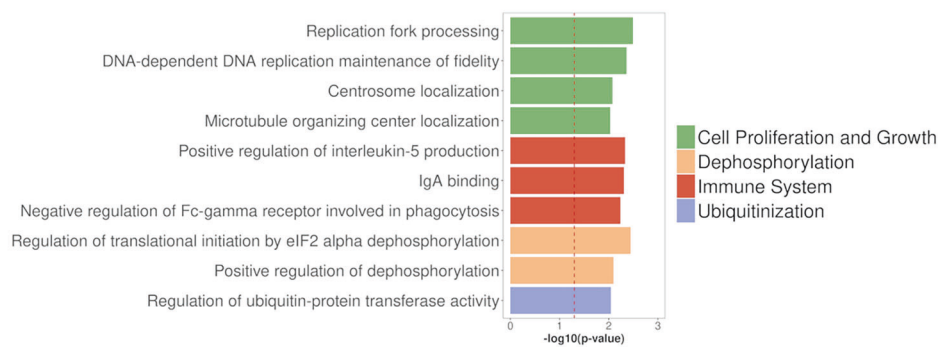
Transcriptomic analysis of patients with Erdheim-Chester disease revealed alterations in the gene expression profile

After QC, differential gene expression analysis between ECD patients and controls was carried out including 14,745 genes in a final cohort of 66 ECD individuals and 358 unaffected controls (Supplementary Table 2). The results revealed 1484 DEGs, of which 75% showed upregulation and the remaining 25% showed downregulation (Fig. 3, Supplementary Table 8). We identified DEGs that were involved in the RAS-RAF-MEK-ERK and PI3K-AKT-

mTOR signaling pathways, as well as in the TNF superfamily pathway (Supplementary Table 5).

To provide an illustrative picture of the putative functional role of the DEGs, we performed protein-protein interaction (PPI) and GO enrichment analyses. The protein molecular network exhibited significantly more interactions than expected (PPI enrichment, $8.48E-05$). Notably, MAP2K2, MAPK12 and AKT2 proteins represented relevant nodes in the PPI network. GO analysis showed that the DEGs were enriched in pathways related to the immune system, cell growth

A



B

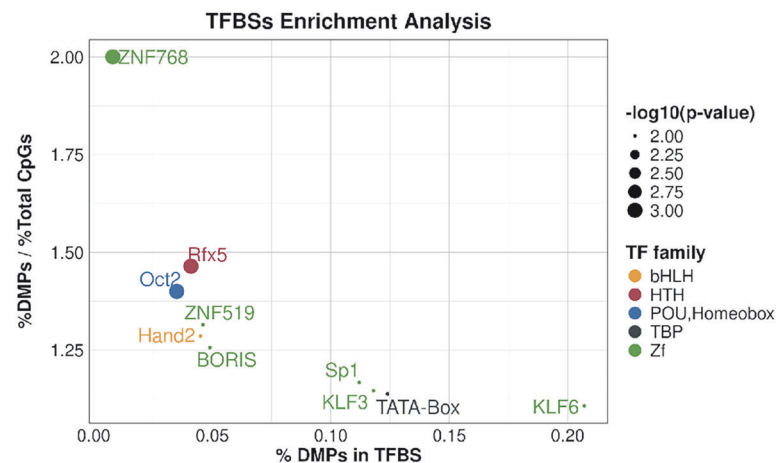


Fig. 2 Results from the enrichment analysis of the differentially methylated positions (DMPs) using EWAS toolkit. A Results of the Gene Ontology (GO) enrichment analysis of DMPs. Most relevant terms are displayed in the plot. The colours of the bars represent the different groups in which the GO terms were classified. **B** Scatter plot displaying significant transcription factors (TFs). X-axis exhibits percentage of DMPs overlapping transcription factor binding sites for each TF. Y-axis represents this value divided by percentage of all analysed CpGs overlapping with the same TF. The colour denotes the transcription factor's family, while the size reflects the significance level in terms of $\log_{10}(p\text{-value})$.

and proliferation, stress response and apoptosis or cell adhesion (Fig. 3, Supplementary Table 9). Interestingly, the most significant enriched pathway was the RAS signaling pathway ($p\text{-value} = 5.85\text{E-}08$). We also identified additional enrichments related to cell growth and proliferation, such as the EGFR and PDGF signaling pathways (Fig. 3, Supplementary Table 9). Interestingly, we observed an enrichment in inflammation mediated by chemokine and cytokine signaling pathway ($p\text{-value} = 8.33\text{E-}05$), T cell activation ($p\text{-value} = 2.23\text{E-}04$), B cell activation ($p\text{-value} = 4.99\text{E-}04$), and toll-like receptor (TLR) ($p\text{-value} = 1.02\text{E-}03$) signaling pathways, all of which could be involved in the inflammatory cascade responsible for tissue damage in ECD.

Integrative approach revealed correlations between alterations in DNA methylation and changes in gene expression

For the integration analysis, we included 35 ECD patients and 146 unaffected controls, that were the samples for which both methylation and transcriptomic data were available and that passed all QCs (Supplementary Table 2). We identified 29 genes differentially expressed in ECD whose expression levels were associated with DNA methylation changes at 46 CpG sites (Table 1). The distribution of CpGs relative to the genes they interact with showed that 83.33% of the CpGs located near or within gene promoters exhibited a negative correlation, while 16.67% revealed a positive correlation. We detected interactions that involved relevant genes in the context of cell division, immune system and tumorigenesis (Table 1). Among the strongest

interactions identified, the upregulation of *RNASET2*, that acts as a tumor suppressor [23], was associated with five distinct CpGs (Table 1). We also detected interactions between genes that might play important roles in the development of ECD. One example was *LRRC14*, that regulates NF- κ B signaling pathway [24]. The upregulation of *LRRC14* correlated with hypermethylation of cg12574437 in ECD patients ($r = 0.35$, $p\text{-value}_{\text{FDR}} = 1.27\text{E-}02$). Moreover, the upregulation of *TGFB1*, which is frequently altered in tumor cells [25], correlated with hypermethylation of cg05217755 in ECD patients ($r = 0.33$, $p\text{-value}_{\text{FDR}} = 4.06\text{E-}02$) (Table 1).

BRAF^{V600E} mutation and MAPK inhibitors do not significantly influence methylation and expression profiles between ECD patients

To investigate the heterogeneity of ECD patients, we conducted a stratified cohort analysis based on BRAF^{V600E} mutation status. We performed a differential methylation analysis, for which 45 BRAF^{V600E}-positive patients, 23 BRAF^{V600E}-negative patients, and 167 unaffected controls were included. Comparisons between BRAF^{V600E}-positive and BRAF^{V600E}-negative patients did not yield any DMP. However, when each BRAF^{V600E} subgroup was compared to controls, we observed substantial methylation changes (BRAF^{V600E}-positive vs. controls: 2446 DMPs; BRAF^{V600E}-negative vs. controls: 2609 DMPs) (Supplementary Tables 10 and 11). Notably, 97% and 91% of these DMPs, respectively, overlapped with those identified in the overall ECD

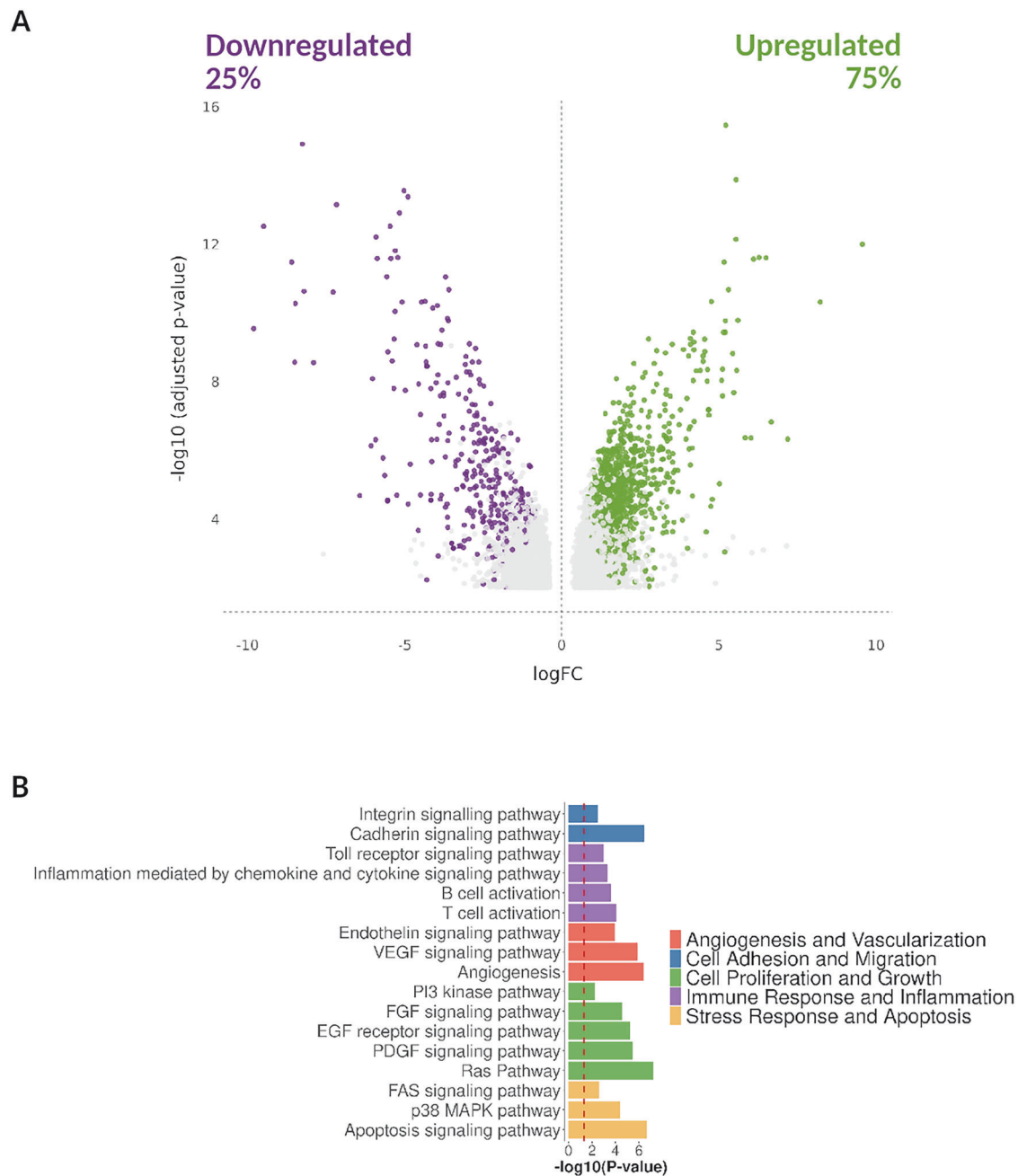


Fig. 3 Results from the comparison of gene expression patterns between patients with Erdheim–Chester disease and controls. A Volcano plot of the transcriptomic study results. False discovery rate (FDR) values are represented on the $-\log_{10}$ scale in the y-axis. The effect size and direction obtained for each gene is depicted in the x-axis through the log fold change (logFC) value. Orange and blue dots represent upregulated and downregulated differentially expressed genes (DEGs), respectively. **B** Results of the Gene Ontology (GO) enrichment analysis of DEGs. Most relevant terms are displayed in the plot. The colours of the bars represent the different groups in which the GO terms were classified.

vs. control comparison. Additionally, to assess the potential impact of MAPK inhibitor therapy in BRAF^{V600E}-positive patients, we stratified BRAF^{V600E}-positive patients into untreated and treated (23 vs. 22, respectively). No significant differences were observed in their methylation patterns.

For the transcriptomic analysis, cohort stratification included 35 BRAF^{V600E}-positive patients, 12 BRAF^{V600E}-negative patients, and 358 unaffected controls. Gene expression profiles were similar between BRAF^{V600E}-positive and BRAF^{V600E}-negative patients, with no DEGs identified. The comparison between BRAF^{V600E}-positive patients and controls revealed 1573 DEGs (Supplementary Table 12), 92% of which overlapped with those from the global ECD vs. control analysis. The

BRAF^{V600E}-negative vs. control comparison identified 315 DEGs (Supplementary Table 13), all of which overlapped with the ECD vs. control DEGs. The lower number of DEGs in the BRAF^{V600E}-negative vs. control analysis may be attributed to reduced statistical power due to the smaller sample size in this comparison. Finally, no significant differences were detected between untreated and treated BRAF^{V600E}-positive patients (22 vs. 13, respectively).

Drug repurposing analysis identified novel potential treatments for Erdheim–Chester disease

In an attempt to identify potential new drugs for ECD based on the data generated in our study, a drug repurposing analysis was

Table 1. Results of the integrative analysis between DNA methylation and gene expression data in Erdheim–Chester disease.

Chr	Gene	CpG	Integration		Methylation		Gene Expression	
			<i>R</i>	<i>P</i> (FDR)	$\Delta\beta$	<i>P</i> (FDR)	logFC	<i>P</i> (FDR)
chr16	<i>ACSF3</i>	cg04879696	−0,34	2,28E−02	−0,01	5,94E−05	1,52	4,76E−07
chr19	<i>CLEC11A</i>	cg10773601	−0,38	1,90E−03	−0,05	6,64E−03	2,34	6,73E−03
		cg20308817	−0,33	4,27E−02	−0,04	6,13E−04		
chr17	<i>DNAH17</i>	cg07125124	0,39	1,38E−03	0,01	1,51E−04	4,67	6,55E−08
		cg16403016	−0,41	2,33E−04	−0,03	2,52E−03		
		cg27174444	0,35	1,62E−02	0,04	1,42E−07		
chr9	<i>EEF1A1P5</i>	cg17246894	−0,35	1,80E−02	0,03	1,17E−09	−2,84	5,72E−06
		cg19777542	0,34	2,96E−02	−0,01	8,80E−05		
chr1	<i>EIF1AXP1</i>	cg16109817	−0,36	8,02E−03	0,01	5,39E−11	−3,65	3,64E−05
chr16	<i>EIF3CL</i>	cg27416312	−0,33	4,88E−02	−0,01	5,58E−03	2,78	1,92E−05
chr12	<i>EIF4B</i>	cg01657380	−0,34	2,44E−02	0,01	3,75E−03	−1,00	7,84E−05
chr20	<i>FRG1BP</i>	cg04692312	0,50	6,83E−08	−0,15	8,17E−09	−2,26	1,35E−04
		cg09798387	0,41	3,70E−04	−0,05	1,09E−03		
		cg14709901	0,36	9,01E−03	−0,02	6,18E−03		
		cg15069499	−0,46	3,66E−06	0,09	6,23E−12		
		cg19196320	−0,50	8,43E−08	0,09	2,98E−05		
chr5	<i>HK3</i>	cg05017829	−0,33	3,63E−02	−0,01	5,93E−04	1,56	1,23E−03
chr6	<i>HLA-J</i>	cg20380424	−0,42	1,02E−04	0,05	6,75E−04	−5,25	1,99E−05
		cg20408505	0,38	3,05E−03	−0,06	9,61E−06		
chr6	<i>HLA-K</i>	cg15411272	0,34	2,42E−02	−0,19	8,06E−10	−4,89	3,65E−05
chr9	<i>LINC00963</i>	cg13523245	0,45	9,05E−06	0,03	1,71E−04	1,43	5,16E−04
		cg14854366	−0,41	3,07E−04	−0,04	1,09E−03		
		cg21226933	0,43	7,87E−05	0,02	1,91E−04		
chr9	<i>LINC02908</i>	cg19993487	−0,34	2,46E−02	−0,02	2,29E−03	1,69	3,16E−03
chr8	<i>LRRC14</i>	cg12574437	0,35	1,27E−02	0,02	1,86E−03	1,38	1,02E−04
chr1	<i>LYSMD1</i>	cg01281797	−0,44	3,71E−05	−0,02	2,49E−04	1,73	1,41E−05
chr6	<i>MIR6891</i>	cg08509237	−0,34	2,83E−02	0,01	6,78E−03	−1,57	7,69E−04
chr8	<i>NAPRT</i>	cg22097396	−0,36	9,37E−03	−0,04	3,59E−11	2,32	9,64E−05
		cg25786937	−0,37	6,23E−03	−0,04	1,05E−04		
chr9	<i>NPDC1</i>	cg26581729	−0,35	1,33E−02	−0,03	6,13E−04	2,53	6,54E−05
chr11	<i>PRR33</i>	cg17501754	0,34	2,13E−02	0,01	4,64E−03	9,57	1,01E−12
chr19	<i>PWWP3A</i>	cg14007004	0,36	7,83E−03	0,04	5,10E−03	0,99	1,33E−04
chr4	<i>RAC1P2</i>	cg09100767	0,36	8,02E−03	−0,02	5,28E−04	−4,11	7,16E−11
chr6	<i>RNASET2</i>	cg01075399	−0,39	1,01E−03	−0,03	4,08E−03	1,53	3,99E−04
		cg20406979	−0,54	1,41E−09	−0,05	1,50E−05		
		cg20486651	−0,36	9,51E−03	−0,07	1,13E−04		
		cg24398081	0,35	1,82E−02	0,01	2,91E−03		
		cg26887226	0,36	9,04E−03	0,03	2,37E−03		
chr5	<i>SLC22A5</i>	cg24887267	−0,34	2,04E−02	−0,01	2,13E−03	1,24	1,64E−04
chr14	<i>SLC25A29</i>	cg14064024	−0,57	2,26E−11	−0,05	2,72E−06	2,00	5,60E−04
chr3	<i>STIMATE-MUSTN1</i>	cg10525161	0,35	1,44E−02	0,01	5,99E−03	6,50	2,49E−12
chr10	<i>STK32C</i>	cg01807317	−0,36	9,47E−03	−0,05	1,28E−05	1,49	6,11E−05
chr16	<i>TBC1D10B</i>	cg16410688	0,33	4,68E−02	0,01	3,73E−04	1,23	5,60E−05
chr19	<i>TGFB1</i>	cg05217755	0,33	4,06E−02	0,01	1,99E−09	1,41	2,44E−05
chr22	<i>TRIOBP</i>	cg16774942	0,33	3,45E−02	0,00	3,30E−18	1,28	4,42E−04
		cg18442977	0,34	2,16E−02	0,00	5,57E−03		

Only significant interactions are showed (i.e., interaction pairs in which both methylation and expression levels were independently associated to the disease and in which CpG-gene interaction had a *p*-value (FDR) < 0.05 in the integrative analysis by MatrixEQTL). $\Delta\beta$, ratio of DNA methylation between cases and controls. Chr, chromosome. logFC, log fold change.

carried out using the proteins encoded by the genes identified in the integrative analysis as well as the proteins that interact with them based on STRING [21]. Among the 109 evaluated proteins, 33 were targeted by different approved drugs (Supplementary Table 14). Interestingly, one of these drugs, cladribine, has been suggested as a treatment option in patients with ECD without the BRAF^{V600E} mutation [26]. Furthermore, other identified drugs, such as fostamatinib, sulfasalazine, and auranofin, have been used in the treatment of IMIDs and/or neoplastic conditions and could be of interest for ECD treatment (Table 2).

DISCUSSION

Over the last decade, advances in the understanding of ECD have significantly improved its diagnosis and treatment, resulting in an increased number of diagnosed cases and a reduction in mortality rates [1, 2, 4]. Nevertheless, major challenges persist in the clinical management of ECD, mainly due to the substantial variability in its clinical and pathological characteristics, which complicates both timely diagnosis and the selection of an optimal treatment strategy [2, 4]. In this context, a comprehensive characterization of the molecular alterations underlying ECD is essential for the identification of robust biomarkers that facilitate early diagnosis and novel therapeutic targets.

In this study, we investigate for the first time the molecular profiles of ECD patients by analyzing their methylome and transcriptome. Our results uncovered over 2500 DMPs and around 1500 DEGs, respectively. These findings emphasized a profound epigenetic and transcriptomic dysregulation in ECD patients. Interestingly, BRAF^{V600E} mutational status and MAPK inhibitors do not significantly influence methylation and expression profiles in ECD patients, underlining that the complexity of ECD pathogenesis cannot be explained exclusively by somatic mutations. Of interest, the integration analysis allowed the identification of a subset of gene expression changes that were linked to methylation abnormalities in ECD.

Somatic mutations affecting the RAS-RAF-MEK-ERK and PI3K-AKT-mTOR pathways are well-established drivers of ECD pathogenesis in a large proportion of patients, highlighting the neoplastic component of the disease [1, 2, 4]. Our findings underscore the significance of neoplastic processes in ECD, shedding light on their impact at both the epigenomic and transcriptomic levels. Enrichment analysis of DMPs and DEGs revealed key pathways regulating cell growth, proliferation, differentiation, and survival. Interestingly, the EGFR signaling pathway activates several major downstream cascades, including the RAS and PI3K pathways [27]. Given that the EGFR pathway has been targeted in cancer therapies [28], it is tempting to hypothesized that it could be considered a potential new therapeutic target for ECD. Moreover, DMPs were enriched in binding sites for ten TFs, seven of which have been previously implicated in cancer (Supplementary Table 7). Their identification in ECD supports the neoplastic component of the disease and highlights novel molecular mechanisms potentially involved in its pathogenesis.

Inflammation is a hallmark of ECD, with over 80% of patients presenting systemic inflammation. However, few studies have focused on understanding the inflammatory component of this disease, which remains poorly understood [4]. Our results highlight the significant role of the immune/inflammatory component in ECD development. Thus, transcriptomic enrichment analysis identified B and T cell activation as relevant pathways in ECD. In this context, Th1 cells have been suggested to play a role in ECD pathogenesis, based on serum molecule levels observed in patients [4]. Interestingly, our findings are the first to implicate B cells as a cellular component potentially involved in the inflammatory processes underlying this disease. In this sense, enrichment analysis of DMPs showed increased regulation of IL-5

Table 2. Summary of the most relevant drugs identified in the drug repurposing analysis.

Associated gene	Target	Drug	Type	Current indication
NAPRT	PNP	Cladribine	Small Molecule	Chronic lymphocytic leukemia, Cutaneous T-cell lymphoma, Relapsing multiple sclerosis, Hairy cell leukemia
LRRC14	CHUK, IKKB	Sulfasalazine	Small Molecule	Rheumatoid arthritis, Crohn's disease, Ulcerative colitis, Proctitis, Polyarticular juvenile rheumatoid arthritis
LRRC14	IKKB	Auranofin	Small Molecule	Rheumatoid arthritis
LRRC14, TGFB1	IKKB, TGFB1, TGFB2	Fostamatinib	Small Molecule	Chronic immune thrombocytopenia

production and IgA binding. IL-5 is essential for B cell differentiation and enhances IgA production via plasma cells [29]. Additionally, OCT2, a TF identified in the enrichment analyses, is involved in B cell regulation and their differentiation into plasma cells, through the IL-5 receptor gene, under T-cell dependent conditions [30, 31]. Therefore, our findings suggest possible alterations in B-cell regulation and differentiation in ECD patients, as highlighted by both expression and methylation results. Notably, ECD tissue lesions typically exhibit low levels of B-cell infiltration. However, it is important to note that our analyses were conducted using whole blood samples. Thus, the observed alterations in B cell-related pathways are more likely to reflect systemic immune dysregulation rather than a direct pathogenic role of B cells in tissue damage. In this context, future studies will be essential to elucidate the specific contribution of B cells to ECD pathophysiology.

One of the major challenges in understanding ECD pathogenesis is the unclear relationship between clonal histiocyte proliferation and systemic inflammation. In this context, our results highlight pathways that may shed light on this connection. First, the enrichment of the integrin signaling pathway, which is essential for cell–extracellular matrix interactions [32], could suggest that integrins may facilitate histiocyte proliferation, adhesion, and tissue infiltration in ECD. Second, the enrichment of negative regulation of Fc-gamma receptor-mediated phagocytosis may reflect impaired phagocytic activity, a feature characteristic of senescent cells [33]. This finding aligns with previous studies describing the expression of senescence markers in BRAF^{V600E}-mutated histiocytes with a potential inflammatory role in ECD [34]. Third, the enrichment of the inflammation mediated by chemokine and cytokine signaling pathway underscores the active role of these soluble mediators in maintaining a pro-inflammatory environment and promoting histiocyte accumulation.

Interestingly, our study has also revealed novel insights involving the NF-κB pathway in ECD pathogenesis. In this sense, the integrative analysis pointed to *LRRCT4*, a gene that negatively regulates TLR-mediated NF-κB signaling through its interaction with IKBKB [24]. Specifically, *LRRCT4* is involved in TLR7/8 cascade, which participates in tumor growth and surveillance, and promote histiocytosis [35, 36]. Additionally, the integrative analysis identified *RNASET2* and *TGFB1*, two genes that interact with TLR8 and NF-κB, respectively [37, 38]. The methylome and transcriptome results also reinforce this idea. The transcriptomic analysis revealed enrichment of the TLR and EGFR signaling pathways, with EGFR being a known activator of NF-κB signaling [39]. Furthermore, the TF enrichment analysis identified Sp1 and KLF6, two regulators of the NF-κB pathway [40–42]. Notably, previous studies have reported a cross-regulation between the MAPK and NF-κB pathways, highlighting their interplay in cancer progression [42]. Hence, NF-κB pathway may represent an additional mechanism that could contribute to the link between the clonal component and the inflammatory processes of ECD. Finally, it is noteworthy that NF-κB is critical for B cell development and activation [43], which aligns with our findings suggesting B cell involvement in the pathogenesis of ECD. Considering all the above, we propose the NF-κB pathway as a potentially critical pathway in the development of this disease.

ECD management remains complex, and the search for effective treatments represents a significant hurdle. In this regard, drug repurposing is a valuable strategy, as it can shorten the drug development timeline and enhance the success rate of drug approval [44]. The drug repositioning analysis identified sulfasalazine, auranofin, and fostamatinib as potential therapeutic candidates for ECD. Interestingly, all these drugs target IKBKB, a key member of the NF-κB pathway. Notably, fostamatinib is a kinase inhibitor that acts on B-cell activation, T-cell activation, and signal transduction by Fc-gamma receptors [45, 46], which are enriched pathways in ECD according to our results. This drug is

indicated for chronic immune thrombocytopenia and is under clinical trials for B- and T-cell lymphomas, and different IMiDs (NCT01499303, NCT00798096, NCT02612558, NCT01197521, NCT01197534, NCT01197755). Collectively, our findings suggest that these drugs may benefit ECD patients, but further experimental and clinical validation is essential.

In conclusion, this study marks a significant step in understanding ECD pathogenesis. We identified substantial disruptions in multiple molecular pathways, particularly those associated with neoplastic mechanisms and inflammatory processes. Moreover, we have identified novel mechanisms that may play critical roles in disease progression. Outstandingly, the identification of B cells as a pivotal cellular component in ECD pathogenesis, along with the involvement of the NF-κB pathway, underscores new avenues for disease management. Furthermore, the identification of candidate drugs that have been successfully used in diseases with similar features to ECD represents a crucial step toward improving therapeutic options for these patients.

DATA AVAILABILITY

The data underlying this study are available upon request from the corresponding author. Due to privacy or ethical restrictions, they are not publicly accessible.

REFERENCES

1. Haroche J, Cohen-Aubart F, Amoura Z. Erdheim-Chester disease. *Blood*. 2020;135:1311–8.
2. Goyal G, Heaney ML, Collin M, Cohen-Aubart F, Vaglio A, Durham BH, et al. Erdheim-Chester disease: consensus recommendations for evaluation, diagnosis, and treatment in the molecular era. *Blood*. 2020;135:1929–45.
3. Pegoraro F, Mazzariol M, Trambusti I, Bakhshi S, Mallick S, Dunkel U, et al. Childhood-onset Erdheim-Chester disease in the molecular era: clinical phenotypes and long-term outcomes of 21 patients. *Blood*. 2023;142:1167–71.
4. Pegoraro F, Papo M, Maniscalco V, Charlotte F, Haroche J, Vaglio A. Erdheim-Chester disease: a rapidly evolving disease model. *Leukemia*. 2020;34:2840–57.
5. McClain KL, Bigenwald C, Collin M, Haroche J, Marsh RA, Merad M, et al. Histiocytic disorders. *Nat Rev Disease Primers*. 2021;7:73.
6. Martínez-López J, Márquez A, Pegoraro F, Ortiz-Fernández L, Acosta-Herrera M, Kerick M, et al. Genome-wide association study identifies the first germline genetic variant associated with Erdheim-Chester disease. *Arthritis Rheumatol*. 2024;76:141–5.
7. Mazzone R, Zwergel C, Artico M, Taurone S, Ralli M, Greco A, et al. The emerging role of epigenetics in human autoimmune disorders. *Clin Epigenetics*. 2019;11:34.
8. Esteller M, Dawson MA, Kadoch C, Rassool FV, Jones PA, Baylin SB. The epigenetic hallmarks of cancer. *Cancer Discov*. 2024;14:1783–809.
9. Hanahan D. Hallmarks of cancer: new dimensions. *Cancer Discov*. 2022;12:31–46.
10. Berdasco M, Esteller M. Clinical epigenetics: seizing opportunities for translation. *Nat Rev Genetics*. 2019;20:109–27.
11. Ballestar E, Sawalha AH, Lu Q. Clinical value of DNA methylation markers in autoimmune rheumatic diseases. *Nat Rev Rheumatol*. 2020;16:514–24.
12. Tejedor JR, Bueno C, Vinyoles M, Petazzi P, Agraz-Doblas A, Cobo I, et al. Integrative methylome-transcriptome analysis unravels cancer cell vulnerabilities in infant MLLrearranged B cell acute lymphoblastic leukemia. *J Clin Invest*. 2021;131:e138833.
13. Barturen G, Babaei S, Català-Moll F, Martínez-Bueno M, Makowska Z, Martorell-Marugán J, et al. Integrative analysis reveals a molecular stratification of systemic autoimmune diseases. *Arthritis Rheumatol*. 2021;73:1073–85.
14. Martínez-López J, Ortiz-Fernández L, Estupiñán-Moreno E, Kerick M, Andrés-León E, Terron-Camero LC, et al. A strong dysregulated myeloid component in the epigenetic landscape of systemic sclerosis: an integrated DNA methylome and transcriptome analysis. *Arthritis Rheumatol*. 2024;77:439–49.
15. Go RS, Jacobsen E, Baiocchi R, Buhtoiarov I, Butler EB, Campbell PK, et al. Histiocytic neoplasms. *J Natl Compr Cancer Netw*. 2021;19:1277–303.
16. Barturen G, Beretta L, Cervera R, Van Vollenhoven R, Alarcón-Riquelme ME. Moving towards a molecular taxonomy of autoimmune rheumatic diseases. *Nat Rev Rheumatol*. 2018;14:75–93.
17. Ritchie ME, Phipson B, Wu D, Hu Y, Law CW, Shi W, et al. Limma powers differential expression analyses for RNA-sequencing and microarray studies. *Nucleic Acids Res*. 2015;43:e47.
18. Campos-Laborie FJ, Risueño A, Ortiz-Estévez M, Rosón-Burgo B, Droste C, Fontanillo C, et al. DECO: Decompose heterogeneous population cohorts for patient

- stratification and discovery of sample biomarkers using omic data profiling. *Bioinformatics*. 2019;35:3651–62.
19. Shabalín AA. Matrix eQTL: Ultra fast eQTL analysis via large matrix operations. *Bioinformatics*. 2012;28:1353–8.
 20. Wishart DS, Feunang YD, Guo AC, Lo EJ, Marcu A, Grant JR, et al. DrugBank 5.0: a major update to the DrugBank database for 2018. *Nucleic Acids Res*. 2018;46:D1074–82.
 21. Szklarczyk D, Franceschini A, Wyder S, Forslund K, Heller D, Huerta-Cepas J, et al. STRING v10: Protein-protein interaction networks, integrated over the tree of life. *Nucleic Acids Res*. 2015;43:D447–52.
 22. Karlsson M, Zhang C, Méar L, Zhong W, Digre A, Katona B, et al. A single-cell type transcriptomics map of human tissues. *Sci Adv*. 2021;7:eab2169.
 23. Bruno A, Noonan DM, Valli R, Porta G, Taramelli R, Mortara L, et al. Human RNASET2: a highly pleiotropic and evolutionary conserved tumor suppressor gene involved in the control of ovarian cancer pathogenesis. *Int J Mol Sci*. 2022;23:9074.
 24. Wu C, Yang Y, Ou J, Zhu L, Zhao W, Cui J. LRRCL4 attenuates Toll-like receptor-mediated NF- κ B signaling through disruption of IKK complex. *Exp Cell Res*. 2016;347:65–73.
 25. de Streele G, Lucas S. Targeting immunosuppression by TGF- β 1 for cancer immunotherapy. *Biochem Pharmacol*. 2021;192:114697.
 26. Goyal G, Shah MV, Call TG, Litzow MR, Hogan WJ, Go RS. Clinical and radiologic responses to cladribine for the treatment of Erdheim-Chester disease. *JAMA Oncol*. 2017;3:1253–6.
 27. Runkle KB, Kharbanda A, Stypulkowski E, Cao XJ, Wang W, Garcia BA, et al. Inhibition of DHHC20-mediated EGFR palmitoylation creates a dependence on EGFR signaling. *Mol Cell*. 2016;62:385–96.
 28. Hawash M. Advances in cancer therapy: a comprehensive review of CDK and EGFR inhibitors. *Cells*. 2024;13:1656.
 29. Takatsu K, Nakajima H. IL-5 and eosinophilia. *Current Opinion in Immunology*. 2008;20:288–94.
 30. Emslie D, Costa KD, Hasbold J, Metcalf D, Takatsu K, Hodgkin PO, et al. Oct2 enhances antibody-secreting cell differentiation through regulation of IL-5 receptor α chain expression on activated B cells. *J Exp Med*. 2008;205:409–21.
 31. Hodson DJ, Shaffer AL, Xiao W, Wright GW, Schmitz R, Phelan JD, et al. Regulation of normal B-cell differentiation and malignant B-cell survival by OCT2. *Proc Natl Acad Sci USA*. 2016;113:E2039–46.
 32. Liu F, Wu Q, Dong Z, Liu K. Integrins in cancer: emerging mechanisms and therapeutic opportunities. *Pharmacol Ther*. 2023;247:108458.
 33. Wang L, Hong W, Zhu H, He Q, Yang B, Wang J, et al. Macrophage senescence in health and diseases. *Acta Pharm Sin B*. 2024;14:1508–24.
 34. Cangi MG, Biavasco R, Cavalli G, Grassini G, Dal-Cin E, Campochiaro C, et al. BRAFV600E-mutation is invariably present and associated to oncogene-induced senescence in Erdheim-Chester disease. *Ann Rheum Dis*. 2015;74:1596–602.
 35. Sun H, Li Y, Zhang P, Xing H, Zhao S, Song Y, et al. Targeting toll-like receptor 7/8 for immunotherapy: recent advances and perspectives. *Biomark Res*. 2022;10:89.
 36. Shibata T, Sato R, Taoka M, Saitoh SI, Komine M, Yamaguchi K, et al. TLR7/8 stress response drives histiocytosis in SLC29A3 disorders. *J Exp Med*. 2023;220:e20230054.
 37. Greulich W, Wagner M, Gaidt MM, Stafford C, Cheng Y, Linder A, et al. TLR8 is a sensor of RNase T2 degradation products. *Cell*. 2019;179:1264–75.e13.
 38. Freudlsperger C, Bian Y, Contag Wise S, Burnett J, Coupar J, Yang X, et al. TGF- β and NF- κ B signal pathway cross-talk is mediated through TAK1 and SMAD7 in a subset of head and neck cancers. *Oncogene*. 2013;32:1549–59.
 39. Nam YW, Shin JH, Kim S, Hwang CH, Lee CS, Hwang G, et al. EGFR inhibits TNF- α -mediated pathway by phosphorylating TNFR1 at tyrosine 360 and 401. *Cell Death Differ*. 2024;31:1318–32.
 40. Masilamani AP, Ferrarese R, Kling E, Thudi NK, Kim H, Scholtens DM, et al. KLF6 depletion promotes NF- κ B signaling in glioblastoma. *Oncogene*. 2017;36:3562–75.
 41. Zhang Y, Chen HX, Zhou SY, Wang SX, Zheng K, Xu DD, et al. Sp1 and c-Myc modulate drug resistance of leukemia stem cells by regulating survivin expression through the ERK-MSK MAPK signaling pathway. *Mol Cancer*. 2015;14:56.
 42. Oeckinghaus A, Hayden MS, Ghosh S. Crosstalk in NF- κ B signaling pathways. *Nature Immunol*. 2011;12:695–708.
 43. Guldenpfennig C, Teixeira E, Daniels M. NF- κ B's contribution to B cell fate decisions. *Front Immunol*. 2023;14:1214095.
 44. Minikel EV, Painter JL, Dong CC, Nelson MR. Refining the impact of genetic evidence on clinical success. *Nature*. 2024;629:624–9.
 45. Riccaboni M, Bianchi I, Petrillo P. Spleen tyrosine kinases: Biology, therapeutic targets and drugs. *Drug Discov Today*. 2010;15:517–30.
 46. Braselmann S, Taylor V, Zhao H, Wang S, Sylvain C, Baluom M, et al. R406, an orally available spleen tyrosine kinase inhibitor blocks Fc receptor signaling and reduces immune complex-mediated inflammation. *J Pharm Exp Ther*. 2006;319:998–1008.

ACKNOWLEDGEMENTS

We thank Sofia Vargas for her excellent technical assistance, the PRECISEADS consortium for providing the control data, all patients and control donors for their essential collaboration and the 2021 ECD Global Alliance grant.

AUTHOR CONTRIBUTIONS

Contribution: MCM, AV and JM conceived and designed the study; FP, FC, MP, FCA, ZA, JH and AV recruited patients and provided clinical data; FP and AV centralized and interpreted clinical data; MCM, JML, IRM, AM, LOF, MAH, MK, and EAL analyzed and interpreted data; MCM, AV, and JM wrote the manuscript; and all authors have read and approved the final manuscript.

FUNDING INFORMATION

This work was supported by the project “Genome-wide and epigenome-wide association study in patients with Erdheim-Chester Disease,” funded by Histio UK. M.C.-M is beneficiary of a Juan de la Cierva 2022 postdoctoral fellowship (reference number JDC2022-048561-I) funded by MCIN/AEI/ 10.13039/501100011033 and European Union NextGenerationEU/PRTR. J.M.L. was supported by a predoctoral contract in health related research (PFIS) (FI23/00231) from ISCIII. I.R.M. was supported by the program FPU (FPU21/02746) funded by the Spanish Ministry of Science Innovation and Universities. L.O.F. is recipient of a Ramon y Cajal fellowship [RYC2022-036635-I] funded by MICIU/AEI/10.13039/501100011033 and by ESF+.

COMPETING INTERESTS

The authors declare no competing interests.

ETHICS APPROVAL AND CONSENT TO PARTICIPATE

All methods were performed in accordance with relevant guidelines and regulations. The study was approved by the CSIC Ethics Committee, and written informed consent was obtained from all participants, in accordance with the Declaration of Helsinki. Samples were irreversibly anonymized before analysis.

ADDITIONAL INFORMATION

Supplementary information The online version contains supplementary material available at <https://doi.org/10.1038/s41375-025-02742-z>.

Correspondence and requests for materials should be addressed to Miriam Cerván-Martín.

Reprints and permission information is available at <http://www.nature.com/reprints>

Publisher's note Springer Nature remains neutral with regard to jurisdictional claims in published maps and institutional affiliations.



Open Access This article is licensed under a Creative Commons Attribution-NonCommercial-NoDerivatives 4.0 International License, which permits any non-commercial use, sharing, distribution and reproduction in any medium or format, as long as you give appropriate credit to the original author(s) and the source, provide a link to the Creative Commons licence, and indicate if you modified the licensed material. You do not have permission under this licence to share adapted material derived from this article or parts of it. The images or other third party material in this article are included in the article's Creative Commons licence, unless indicated otherwise in a credit line to the material. If material is not included in the article's Creative Commons licence and your intended use is not permitted by statutory regulation or exceeds the permitted use, you will need to obtain permission directly from the copyright holder. To view a copy of this licence, visit <http://creativecommons.org/licenses/by-nc-nd/4.0/>.

© The Author(s) 2025